Engineered Endolysin-Based "Artilysins" To Combat Multidrug-Resistant Gram-Negative Pathogens

Yves Briers,[a] Maarten Walmagh,[a] Victor Van Puyenbroeck,[a] Anneleen Cornelissen,[a] William Cenens,[b] Abram Aertsen,[b] Hugo Oliveira,[c] Joana Azeredo,[c] Gunther Verween,[d] Jean-Paul Pirnay,[d] Stefan Miller,[e] Guido Volckaert,[a] Rob Lavigne[a]

Laboratory of Gene Technology, KU Leuven, Leuven, Belgium[a]; Laboratory of Food Microbiology, KU Leuven, Leuven, Belgium[b]; Centre of Biological Engineering, University of Minho, Braga, Portugal[c]; Laboratory for Molecular and Cellular Technology, Queen Astrid Military Hospital, Brussels, Belgium[d]; Lisando GmbH, Regensburg, Germany[e]

Y.B. and M.W. contributed equally to this work.

ABSTRACT **The global threat to public health posed by emerging multidrug-resistant bacteria in the past few years necessitates the development of novel approaches to combat bacterial infections. Endolysins encoded by bacterial viruses (or phages) represent one promising avenue of investigation. These enzyme-based antibacterials efficiently kill Gram-positive bacteria upon contact by specific cell wall hydrolysis. However, a major hurdle in their exploitation as antibacterials against Gram-negative pathogens is the impermeable lipopolysaccharide layer surrounding their cell wall. Therefore, we developed and optimized an approach to engineer these enzymes as outer membrane-penetrating endolysins (Artilysins), rendering them highly bactericidal against Gram-negative pathogens, including *Pseudomonas aeruginosa* and *Acinetobacter baumannii*. Artilysins combining a polycationic nonapeptide and a modular endolysin are able to kill these (multidrug-resistant) strains *in vitro* with a 4 to 5 log reduction within 30 min. We show that the activity of Artilysins can be further enhanced by the presence of a linker of increasing length between the peptide and endolysin or by a combination of both polycationic and hydrophobic/amphipathic peptides. Time-lapse microscopy confirmed the mode of action of polycationic Artilysins, showing that they pass the outer membrane to degrade the peptidoglycan with subsequent cell lysis. Artilysins are effective *in vitro* (human keratinocytes) and *in vivo* (*Caenorhabditis elegans*).**

IMPORTANCE **Bacterial resistance to most commonly used antibiotics is a major challenge of the 21st century. Infections that cannot be treated by first-line antibiotics lead to increasing morbidity and mortality, while millions of dollars are spent each year by health care systems in trying to control antibiotic-resistant bacteria and to prevent cross-transmission of resistance. Endolysins—enzymes derived from bacterial viruses—represent a completely novel, promising class of antibacterials based on cell wall hydrolysis. Specifically, they are active against Gram-positive species, which lack a protective outer membrane and which have a low probability of resistance development. We modified endolysins by protein engineering to create Artilysins that are able to pass the outer membrane and become active against *Pseudomonas aeruginosa* and *Acinetobacter baumannii*, two of the most hazardous drug-resistant Gram-negative pathogens.**

Received 3 June 2014 **Accepted** 9 June 2014 **Published** 1 July 2014

Citation Briers Y, Walmagh M, Van Puyenbroeck V, Cornelissen A, Cenens W, Aertsen A, Oliveira H, Azeredo J, Verween G, Pirnay J, Miller S, Volckaert G, Lavigne R. 2014. Engineered endolysin-based "Artilysins" to combat multidrug-resistant gram-negative pathogens. mBio 5(4):e01379-14. doi:10.1128/mBio.01379-14.

Editor Roger Hendrix, University of Pittsburgh

Address correspondence to Rob Lavigne, rob.lavigne@kuleuven.be.

Endolysins are produced by bacteriophages at the end of their lytic replication cycle to hydrolyze the bacterial cell wall for progeny release. In the last decade, it has been extensively demonstrated that the addition of recombinant purified endolysin to susceptible Gram-positive bacteria, including *Staphylococcus*, *Streptococcus*, and *Bacillus* species, kills the bacteria through cell lysis, both *in vitro* and in various animal infection models of human disease (1–4). Their rapid action, high specificity, nontoxicity, high efficiency, and low probability of resistance development make them promising, novel enzyme-based antibacterials (5). The expansion of endolysins as antibacterials against important Gram-negative pathogens is hindered by the outer membrane. Although some endolysins show limited membrane-destabilizing properties (6, 7), this outer membrane poses a highly effective permeability barrier for the passage of harmful compounds, including endolysins and many other antibacterial compounds (8). We have previously shown that the use of high hydrostatic pressure (in the range of 150 to 200 MPa) (9) or outer membrane permeabilizers (10) strongly increases the access of endolysins to the Gram-negative peptidoglycan layer. In this study, we developed an efficient methodology of protein engineering of endolysins to generate highly antibacterial, outer membrane-penetrating endolysins termed Artilysins independently of protein transport systems (11). We show that Artilysins cause 4 to 5 log killing of different (clinically relevant) Gram-negative species *in vitro* and are also effective *in vivo*.

RESULTS

Artilysins: proof of concept. The rationale behind Artilysins is based on the modification of endolysins with lipopolysaccharide (LPS)-destabilizing peptides. The LPS layer is stabilized through ionic interactions between divalent cations and phosphate groups and hydrophobic stacking of the lipid A moiety (12). Seven peptides were selected for their (putative) LPS-destabilizing activity based on different physicochemical properties (cationic, hydrophobic or amphipathic) that interfere with these stabilizing forces (see Table S1 in the supplemental material) (13–16). To test this engineering concept, the two most active endolysins (OBPgp279 and PVP-SE1gp146) from our collection of characterized endolysins (7) were used. OBPgp279 originates from *Pseudomonas fluorescens* phage OBP (phiKZ-like; *Myoviridae*) and PVP-SE1gp146 from *Salmonella enterica* serovar Enteritidis phage PVP-SE1 (rV5-like; *Myoviridae*). Both endolysins feature a modular structure with one (PVP-SE1gp146) or two (OBPgp279) N-terminal peptidoglycan-binding (PBD-like) domains and a C-terminal catalytic domain (glycoside hydrolase 19-like family, lysozyme-like superfamily). This domain configuration is rare among endolysins targeting Gram-negative peptidoglycan and is associated with strongly increased enzymatic activity (7, 17, 18). In addition, OBPgp279 has a moderate intrinsic antibacterial effect on *Pseudomonas aeruginosa* (1.10 log reduction) (7). Fourteen different Artilysins (LoGT-001 to LoGT-014) (Fig. 1; see also Tables S2 and S3 in the supplemental material) were produced and purified, the effect of the respective fusions on protein yield was determined (see Table S4), and the antibacterial activity of the different Artilysins against *P. aeruginosa*, *Escherichia coli*, and *Salmonella enterica* serovar Typhimurium was evaluated (see Table S5). The fusion of each LPS-destabilizing peptide to endolysin PVP-SE1gp146 resulted in an enhanced bactericidal activity against *P. aeruginosa* in comparison to wild-type PVP-SE1gp146, but the effect was most prominent for the polycationic nonapeptide (PCNP). The latter is the only peptide that also increases the intrinsic antibacterial effect of OBPgp279, whereas the other peptides appear to inhibit this intrinsic antibacterial effect (Fig. 2A). The highest reduction was obtained with LoGT-001, combining the PCNP tag and OBPgp279, with a 2.61 ± 0.09 log reduction in only 30 min. Thus, the PCNP tag emerged as the most appropriate peptide to confer antibacterial activity to (otherwise nonantibacterial) endolysins.

We also performed the same experiment in the presence of 0.5 mM EDTA, an outer membrane permeabilizer that shows strong synergy with endolysins (10). For both LoGT-001 and LoGT-008, combining the PCNP tag with OBPgp279 and PVP-SE1gp146, respectively, the synergy with EDTA is not compromised by the modification: both the fusion to the PCNP tag and the addition of a low concentration of EDTA confer antibacterial activity against *P. aeruginosa* PAO1 and Br667 (a multidrug-resistant clinical isolate [19]) to the wild-type endolysins or further improve this activity. A maximal reduction of *P. aeruginosa* PAO1, at 5.38 ± 0.19 log, was observed with LoGT-001 (Fig. 2B). This indicates that the PCNP tag has a mode of action different from that of EDTA. This synergy constitutes a potential benefit for the topical applicability of Artilysins. Although *E. coli* and *S.* Typhimurium were also most strongly affected by PCNP-fused endolysins, the general effect was here significantly smaller, with maximal reductions of 1.70 ± 0.05 (*E. coli*) and 0.91 ± 0.04 (*S.* Typhimurium) (see Table S5).

Mode of action of Artilysins. We used time-lapse microscopy to observe the mode of killing by a PCNP-fused endolysin. LoGT-008 was mixed with *P. aeruginosa* PAO1 in the presence of 0.5 mM EDTA and immediately incubated on an agar pad for microscopic observation. Within minutes, the first rods lysed abruptly (see movie http://www.biw.kuleuven.be/dp/logt/phagesinteraction/movieS1.avi). Even before observation could start (<1 min), lysis of some cells had likely occurred, as witnessed by the presence of the remaining debris of lysed cells. Other rods lysed one by one at up to 1 h after addition of LoGT-008. The involvement of peptidoglycan degradation in the lysis process was shown by the transient formation of round or lemon-shaped spheroplasts before complete lysis took place. Septal peptidoglycan appeared to be degraded as well, suggested by the fusion of spheroplasts that originate from almost completely constricted cells (Fig. 3). These observations are fully consistent with the Artilysin concept, stating that the LPS layer is disturbed by the polycationic nonapeptide, followed by penetration of the endolysin moiety through the outer membrane and subsequent lysis due to peptidoglycan degradation.

Evaluation of different endolysins as fusion partners. The PCNP tag was also fused to four additional endolysins from our collection, one with a modular structure (201ϕ2-1gp229) and three smaller ones comprising only a single catalytic domain (7, 20) (LoGT-015 to LoGT-018) (Fig. 1; see also Tables S2 and S3 in the supplemental material). We measured the effect of the PCNP fusion on the enzymatic activity of the different endolysins (see Table S6) and analyzed the bactericidal effect of these new Artilysins on *P. aeruginosa* PAO1 and Br667, *Pseudomonas putida*, *Burkholderia pseudomallei*, *E. coli*, and *S.* Typhimurium (Fig. 4; see also Table S7). Despite a (52% to 94%) reduction in enzymatic activity in comparison to the corresponding wild-type endolysins, all PCNP-fused endolysins showed improved antibacterial activity. In addition, modularity—and/or its associated high enzymatic activity (7)—is a key factor for the success of the Artilysin approach. Besides the reductions in the cell counts of *P. putida* (4.89 ± 0.02 log) and *B. pseudomallei* (4.81 ± 0.05 log), the cell count for the multidrug-resistant *P. aeruginosa* Br667 strain was also drastically reduced by 4.27 ± 0.15 log within 30 min using a single dose (1.5 μM) of LoGT-001 in the presence of 0.5 mM EDTA (see Table S7).

Optimization of the Artilysin approach. To further optimize the potential of the PCNP tag, a set of 31 related variations of the same fusion with both endolysins (OBPgp279 and PVP-SE1gp146) was produced (LoGT-019 to LoGT-049) (Fig. 1; see also Tables S2 and S3 in the supplemental material). These variations encompass various linker lengths between the polycationic tag and the endolysin and the N- or C-terminal fusions of the tag to the endolysin, as well as combinatorial double-tag fusions of the PCNP with additional hydrophobic or amphipathic moieties (see Table S1). With the latter variations, we aimed to respond to differences in LPS structure between *P. aeruginosa* and *E. coli* or *S.* Typhimurium with a corresponding shift from ionic interactions to hydrophobic packing as the major LPS stabilization force (21). The effect on protein yield and enzymatic activity (see Table S8) and on their antibacterial effect against *P. aeruginosa*, *E. coli*, *S.* Typhimurium, and *Acinetobacter baumannii*, both in the absence and presence of 0.5 mM EDTA (see Table S9), was ana-

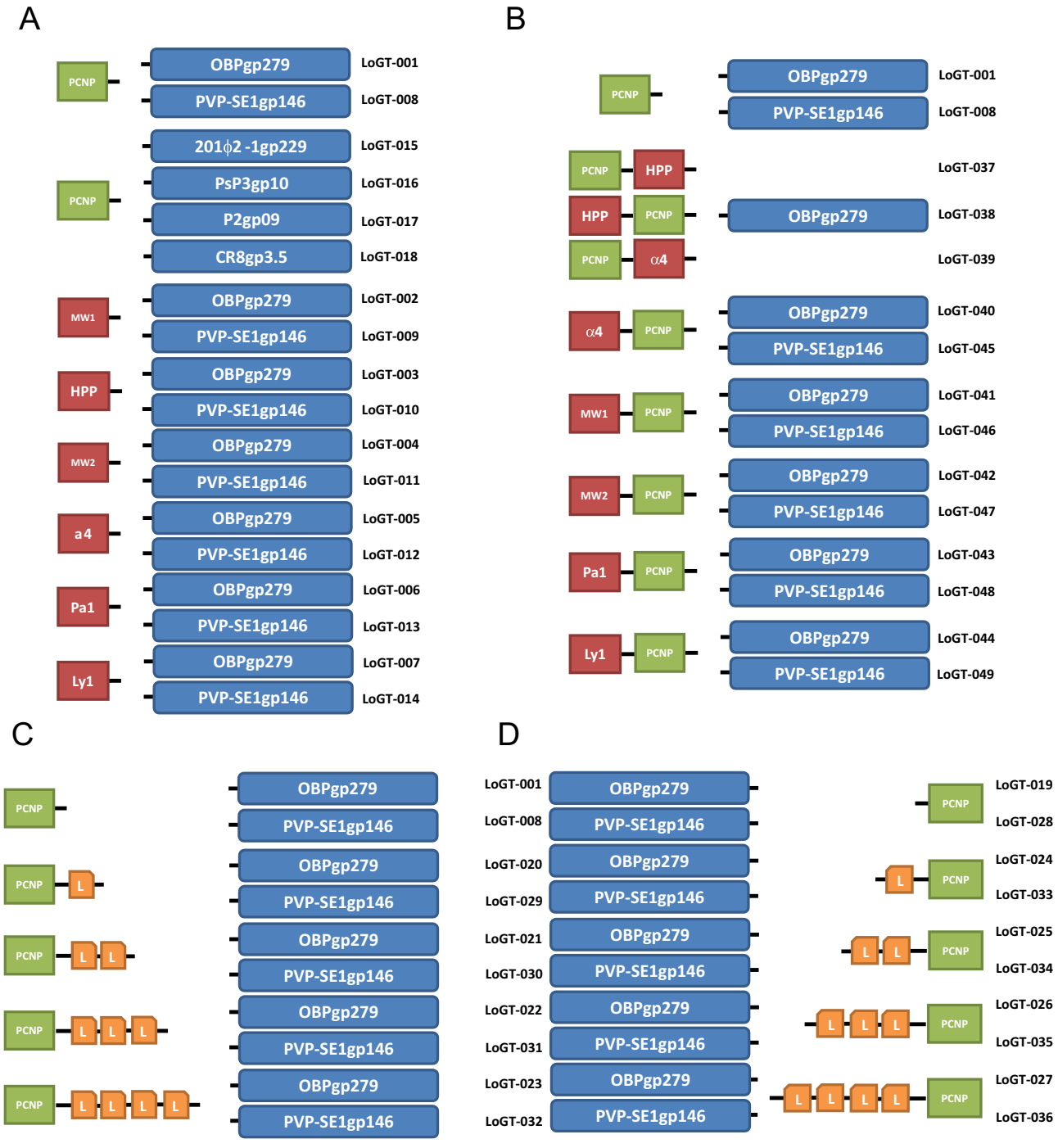

FIG 1 Visual representation of engineered Artilysins. Seven different endolysins (OBPgp279 [YP_004958186.1], PVP-SE1gp146 [YP_004893953.1], phiKZgp144 [NP_803710.1], 201ϕ2-1gp229 [YP_001956952.1], CR8gp3.5 [unpublished], P2gp09 [NP_046765.1], and PsP3gp10 [NP_958065.1) were selected for modification with different peptides. (A) Single N-terminal fusion constructs, (B) double N-terminal fusion constructs, (C) N-terminal extended-linker constructs, (D) C-terminal extended-linker constructs. Abbreviations: PCNP = polycationic peptide, HPP = hydrophobic pentapeptide, Pa1 = Parasin1, Ly1 = lycotoxin1, L = linker unit consisting of GAGA sequence.

lyzed. An increasing length of the linker between the N-terminal PCNP tag and the endolysin results in a slightly higher antibacterial effect against *P. aeruginosa* for Artilysins derived from OBPgp279, with up to a 3.41 ± 0.18 log reduction for LoGT-023 in the absence of EDTA (Fig. 5A). N-terminal fusions generally show higher antibacterial activity than C-terminal fusions (see Table S9). No surviving *P. aeruginosa* cells could be detected after coincubation with the best Artilysins (LoGT-020, LoGT-021, LoGT-022, and LoGT-023) in the presence of 0.5 mM EDTA, which also almost completely eradicated *A. baumannii* (up to 5.33 ± 0.20 log). In the case of *E. coli*, four of eight double-tagged Artilysins (LoGT-037, LoGT-038, LoGT-041, and LoGT-042),

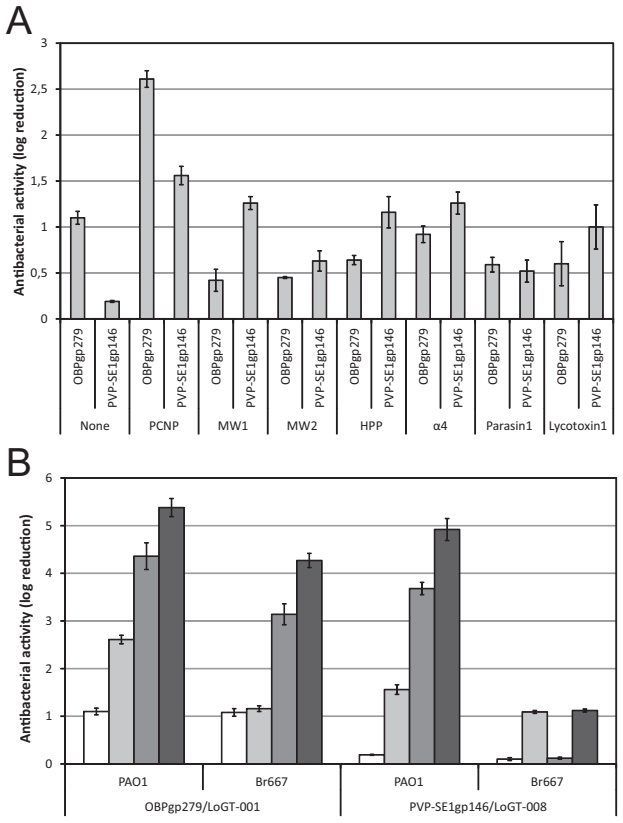

FIG 2 Antibacterial activity of the N-terminal fusion variants of OBPgp279 and PVP-SE1gp146. (A) Fourteen Artilysins with N-terminal fusions of seven different peptides (see Table S1 in the supplemental material) to OBPgp279 and PVP-SE1gp146 are compared to the corresponding unmodified endolysins for their antibacterial activity against *P. aeruginosa* PAO1. This comparison shows the PCNP to be the most effective peptide among the seven peptides tested here. (B) Comparison of the antibacterial activities of two wild-type endolysins (OBPgp279 and PVP-SE1gp146) and their PCNP-tagged Artilysin counterparts (LoGT-001 and LoGT-008, respectively) with and without 0.5 mM EDTA. Activity was tested on *P. aeruginosa* strains PAO1 and multidrug-resistant Br667, both in the absence (wt endolysin, white bars; Artilysin, light gray bars) and presence (wt endolysin, dark gray bars; Artilysin, black bars) of 0.5 mM EDTA. These data show that the PCNP fusion for the antibacterial activity of the endolysin added value while not compromising its synergy with EDTA. Averages and standard deviations of results of three replicates are shown.

combining the PCNP tag with a hydrophobic peptide (HPP; MW1) or amphipathic peptide (MW2), showed an improved bactericidal effect in comparison to the single-tagged Artilysin LoGT-001, with reductions of up to 2.22 ± 0.09 log (Fig. 5B). In the case of *S.* Typhimurium, no improvement could be obtained using the double-tag approach. Altogether, LoGT-023, comprising a 16-amino-acid linker between the N-terminal PCNP tag and OBPgp279, represents the best optimization of LoGT-001, with strong antibacterial activity against *P. aeruginosa* (≥5.50 log) and *A. baumannii* (5.18 ± 0.17 log) and moderate activity against *E. coli* (2.41 ± 0.08 log) and *S.* Typhimurium (1.52 ± 0.07 log) (Fig. 5C).

Artilysins are effective on infected human keratinocytes. Barrier-disrupted skin, such as in burn wounds, is easily infected by different Gram-negative bacteria, most importantly by the opportunistic pathogens *P. aeruginosa* and *A. baumannii* (22). Such topical infections in humans and animals are therefore of primary interest for Artilysin applications. LoGT-008 shows MICs of 4 and 8 μg/ml against *P. aeruginosa* and *A. baumannii*, respectively. In molar concentrations, these values equate to 0.15 and 0.30 μM, which are in the same range as the value for ciprofloxacin (0.5 μM), a common therapeutically used first-line antibiotic for many Gram-negative infections. To evaluate LoGT-008 against *P. aeruginosa* in skin infections, we developed a new human neonatal foreskin keratinocyte model (23). This model relies on a confluent keratinocyte monolayer, infected with *P. aeruginosa* PA14 (10^5 or 10^7 CFU/ml). At 1 h after infection, 2 μM PVP-SE1gp146 or LoGT-008 was added. Keratinocyte viability and bacterial reductions were quantified at 4 h after infection. Both PVP-SE1gp146 and LoGT-008 could fully protect (100%) the monolayer from the otherwise cytotoxic effects upon a PA14 infection with 10^5 CFU/ml (Fig. 6A). This protection is associated with a drastic decrease in bacterial load. A larger bacterial inoculum of 10^7 CFU/ml was found to cause 97% mortality within 4 h. Under these extreme circumstances, a single dose of LoGT-008 could still rescue 27% of the keratinocytes (significantly more than the 14% rescued by the native endolysin; $P < 0.05$). Correspondingly, the bacterial load was reduced significantly ($P < 0.05$) in the presence of LoGT-008 (71% versus 31% for the native endolysin) (Fig. 6B).

Artilysins show *in vivo* antibacterial efficacy. Since the PCNP fusions provide endolysins with *in vitro* antibacterial activity against pseudomonads in both suspension and keratinocyte cultures, we used a *C. elegans* nematode gut infection model (24) to evaluate the *in vivo* efficacy of a PCNP-fused Artilysin, LoGT-008, against bacterial infection. When *C. elegans* grazed on the selected, highly virulent *P. aeruginosa* PA14 strain, 90% of the nematodes were killed within 5 days after infection (see Fig. S1 in the supplemental material). Nematode survival rates were compared after treatment with the native PVP-SE1gp146 endolysin and the corresponding LoGT-008, using ciprofloxacin as a positive control (Fig. 7). In the presence of 0.5 mM EDTA, PVP-SE1gp146 could rescue 40% ± 7% of the infected worms after 5 days. In the same assay, LoGT-008 showed a significant ($P < 0.01$) protective effect in the longer term (63% ± 4% survival) versus 45% ± 5% survival after treatment with ciprofloxacin.

DISCUSSION

The concept of endolysins as antibacterials against Gram-positive pathogens was postulated in 1991 by Gasson (25) and proven in 2001 by Nelson et al., reporting the prevention and elimination of group A streptococcus colonization in the upper respiratory tract of mice (1). Since then, a multitude of endolysins active against diverse Gram-positive pathogens have been described, while Gram-negative targets have been largely neglected (5). We have previously reported the efficacy of a combination of high hydrostatic pressure (9) or outer membrane permeabilizers (10) with endolysins against Gram-negative species. We, and other authors, also described the existence of some endolysins that have moderate intrinsic antibacterial activity against *P. aeruginosa*, most likely because they can interact with and partially pass across the outer membrane barrier (7, 8). In this study, we showed that tailoring highly active, modular phage endolysins with a polycationic peptide turns them in potent antibacterials that are active against a

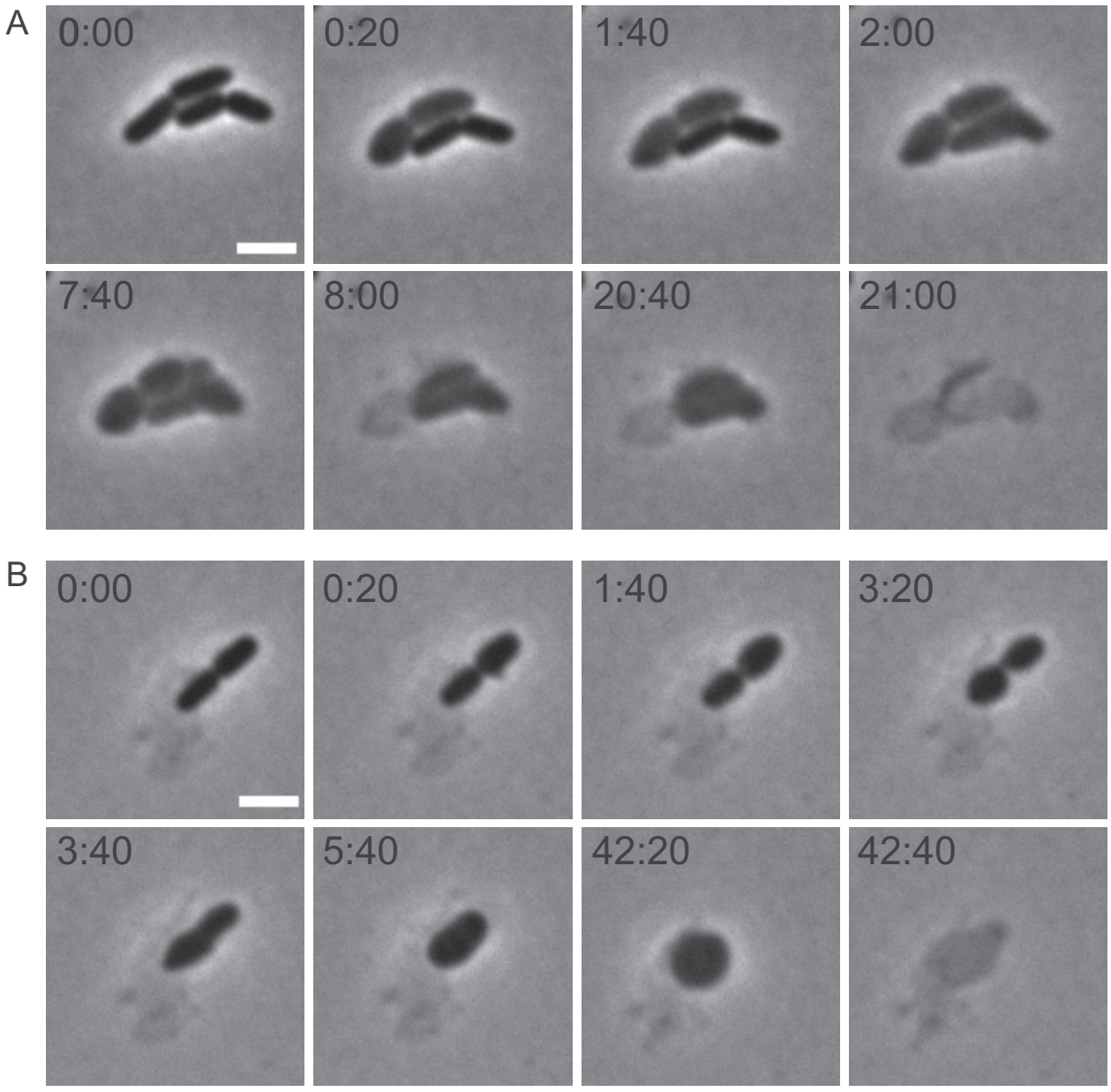

FIG 3 Time-lapse series of the action of LoGT-008 on *P. aeruginosa* PAO1. Cells were mixed with LoGT-008 in the presence of 0.5 mM EDTA and were subsequently recorded using time-lapse microscopy. Time points are indicated (min:s). Scale bar, 2 μm.

broad range of important Gram-negative pathogens. Through this engineering, endolysins acquire autonomous antibacterial activity, and in the case of OBPgp279, which itself possesses intrinsic activity, the antibacterial effect is further enhanced to the same extent as for PVP-SE1gp146. Time-lapse microscopy of cells exposed to LoGT-008 confirmed that cells are indeed killed through cell lysis as a consequence of peptidoglycan degradation. Therefore, the endolysin moiety must have been transferred through the outer membrane, most likely because of the competitive displacement of stabilizing divalent cations of the LPS layer by the polycationic nonapeptide. The reduced enzymatic activity after PCNP fusion does not impede the strong antibacterial activity; however, considering that the most active (modular) endolysins generally show the best antibacterial effect, fusions that maintain the high enzymatic activity of such endolysins may represent a further optimization of novel Artilysins.

Extension of the flexible linkers between the penetrating peptide and the endolysins generally improves the antibacterial activity at up to 3.41 $\pm$ 0.18 against *P. aeruginosa* PAO1 in the case of LoGT-023 in the absence of EDTA. N-terminal fusions perform better than C-terminal fusions of OBPgp279 and PVP-SE1gp146; however, it appears that both the optimal fusion side and linker length are best tested empirically. In specific cases, a combinatorial double-tag approach gives some significant improvements as well, as shown for different Artilysins against *E. coli*. Importantly, in all cases, the strong synergy with EDTA is maintained, giving

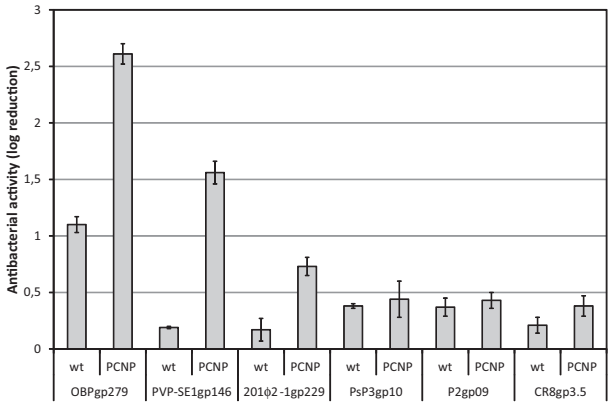

FIG 4 Antibacterial activity of PCNP-Artilysins based on different endolysins. The effect on antibacterial activity of an N-terminal PCNP fusion to three modular (OBPgp279, PVP-SE1gp146, and 201ϕ2-1gp229) and three globular (PsP3gp10, P2gp09, and CR8gp3.5) endolysins is shown for *P. aeruginosa* PAO1. Averages and standard deviations of results of three replicates are shown. wt, wild type.

rise to combinations that reduce cell counts more than 5.50 log (the detection limit) *in vitro*.

The variation in LPS structure appears to be a key determinant for the sensitivity to Artilysins. We specifically focused on the applicability to *P. aeruginosa*, an important emerging multidrug-resistant pathogen. *P. aeruginosa* LPS has a high phosphate content and consequently a higher concentration of divalent cations stabilizing its structure (12). These cations are simultaneously the strength and Achilles' heel of the *P. aeruginosa* LPS layer. EDTA and polycationic peptides act on this same site but through two different mechanisms, chelation and competitive displacement, respectively (26). The lower phosphorylation degree in *E. coli* and *S.* Typhimurium LPS is compensated by increased hydrophobic packing of the lipid A moiety through a higher degree of acylation with longer acyl chains (12). This variation may explain the higher sensitivity of *P. aeruginosa* strains compared to that of *E. coli* and *S.* Typhimurium and the increased activity against *E. coli* of some double tags that combine polycationicity and hydrophobicity/amphipathicity.

Given the proteinaceous nature of Artilysins, they may be considered biodegradable compounds that are less likely to accumulate or induce resistant bacteria in the environment. In contrast, many antibiotics persist in the environment, leading to an increased risk of selecting resistant bacteria, especially when environmental bacteria are exposed to subtherapeutic antimicrobial concentrations (27). This detrimental side effect of many nonbiodegradable antimicrobials may be nonexistent for Artilysins.

Recently, Lukacik and coworkers (11) described an alternative approach to ensure transport of an endolysin across the outer membrane by constructing a hybrid of T4 lysozyme and the FyuA binding domain of pesticin. Reduction of the cell count of about 1 log in 24 h depends on the presence of the TonB-dependent outer membrane transporter FyuA. Besides restriction to *Yersinia* species and uropathogenic *E. coli* strains that express FyuA, this FyuA dependence may also quickly result in resistance development by shutting down *fyuA* expression or the accumulation of point mutations in the *fyuA* genes. Eukaryotic lysozymes have also been subjected to recombinant fusion with diverse peptides or chemical

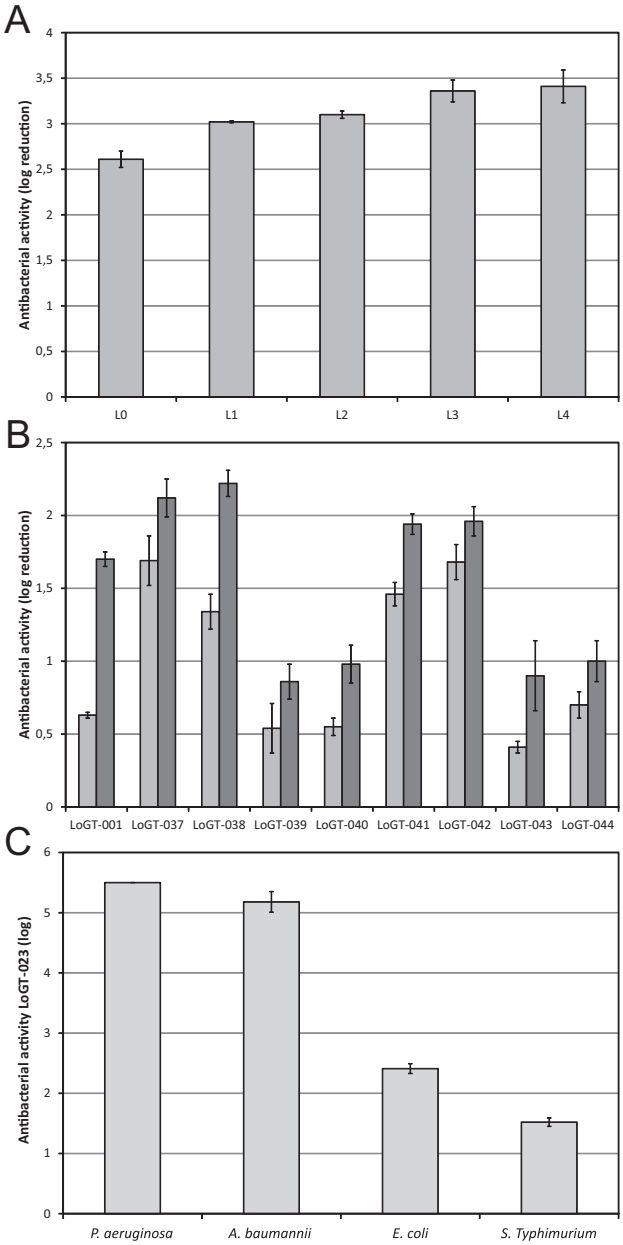

FIG 5 Optimization of PCNP-based Artilysins. (A) The effect of an increasing length of the flexible linker between PCNP and OBPgp279 on the antibacterial activity against *P. aeruginosa* PAO1 is shown. L0, L1, L2, L3, and L4 correspond to intervening amino acid sequences of AGAS, AGAGAS, AGAGAGAGAS, AGAGAGAGAGAGAS, and AGAGAGAGAGAGAGAGAS. (B) The antibacterial activity of Artilysins comprising a tandem of the PCNP peptide and a second peptide as N-terminal fusions to OBPgp279 is compared to that of PCNP-OBPgp279 (LoGT-001) in the absence (light gray) and presence (dark gray) of 0.5 mM EDTA. (C) LoGT-023, comprising a 16-amino-acid flexible linker between the N-terminal PCNP tag and OBPgp279, generally appeared the most effective Artilysin. The antibacterial activity against *P. aeruginosa*, *A. baumannii*, *E. coli*, and *S.* Typhimurium in the presence of 0.5 mM EDTA is shown. Averages and standard deviations of results of three replicates are given.

modifications to render them active against Gram-negative bacteria. Various modifications of the cationic hen egg white lysozyme (HEWL) or human lysozyme have been constructed to

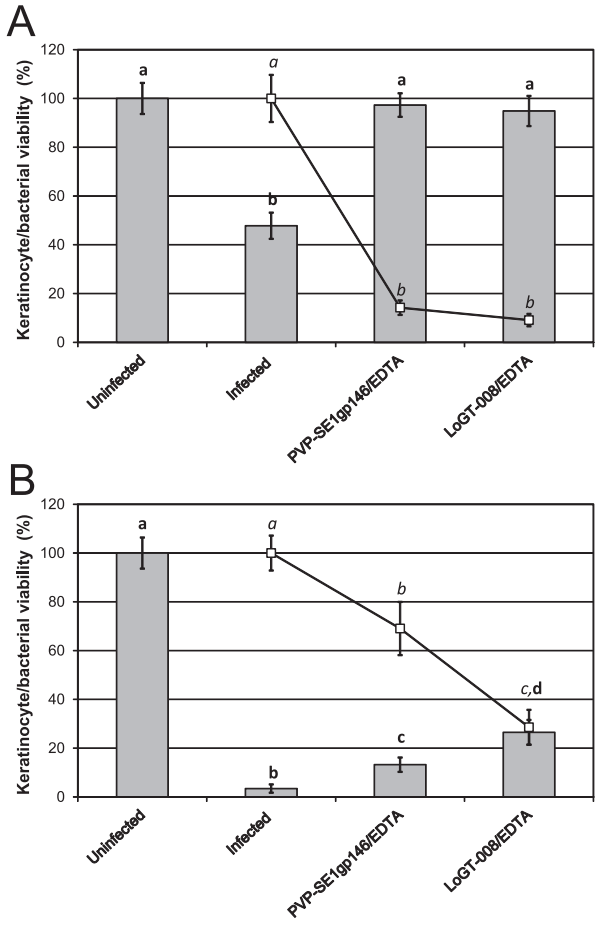

FIG 6 Antibacterial effect of PVP-SE1gp146 and PCNP-PVP-SE1gp146 (LoGT-008) in a *P. aeruginosa* PA14-infected human keratinocyte monolayer. A mixture of 2 μM of PVP-SE1gp146/LoGT-008 and 0.005 mM of EDTA was applied to a 5-day-old confluent keratinocyte monolayer that was infected with 10^5 CFU/ml (A) or 10^7 CFU/ml (B) *P. aeruginosa* PA14 1 h before treatment. Numbers of surviving bacteria (squares) and surviving keratinocytes (bars) were quantified after 4 h of infection. Proportions of surviving bacteria are shown relative to the infected, untreated control results. Significantly different conditions ($P < 0.05$) are indicated with bold (keratinocyte survival) or italic (bacterial survival) letters.

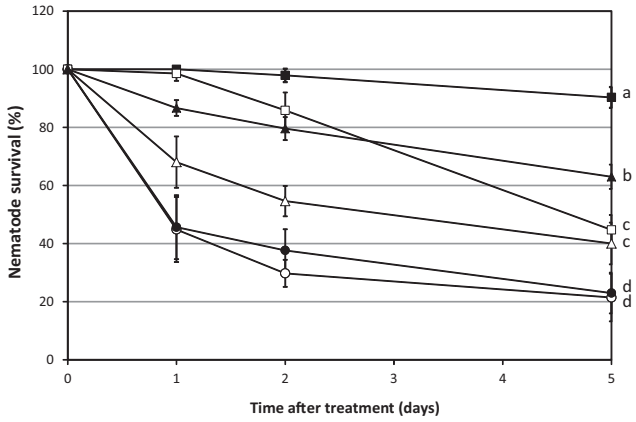

FIG 7 Survival rates of *P. aeruginosa* PA14-infected *C. elegans* SS104 nematodes treated with PVP-SE1gp146 or PCNP-PVP-SE1gp146 (LoGT-008) in combination with EDTA. PVP-SE1gp146 (5× MIC; △) or LoGT-008 (5× MIC; ▲) was added to infected nematodes in the presence of 0.5 mM EDTA. Ciprofloxacin (□; 5× MIC) was used as a positive control for antibacterial activity. Other controls included were untreated PA14-infected nematodes (○), untreated nematodes grown on *E. coli* OP 50 (■), and EDTA-treated infected nematodes (●). A total of 30 infected worms were used for each condition. Nematode viability, in percentages relative to initial values at day 0, was assessed at different time points after compound addition (day 0). Averages and standard deviations of results of three independent experiments are shown. Significantly different conditions ($P < 0.05$) are marked.

increase their hydrophobicity, generating amphitropic proteins with both hydrophilic and lipophilic properties (for a review, see reference 28). These modifications expand the activity range of HEWL to Gram-negative *E. coli*. The highest antibacterial activity was obtained by the covalent attachment of one stearoyl or two palmitoyl acids or by a C-terminal fusion to a hydrophobic pentapeptide (Phe-Phe-Val-Ala-Pro, which has approximately the same length as one palmitoyl acid); however, the maximal bacterial reduction by these HEWL modifications remained below 1 log (29–31).

Multidrug-resistant Gram-negative pathogens are particularly troublesome, because they have intrinsic or acquired resistance to nearly all drugs that can be currently considered for treatment. This worrisome situation also exists, but not to the same extent, for some Gram-positive infections (e.g., *Staphylococcus* and *Enterococcus*). The most prevalent Gram-negative pathogens are *Enterobacteriaceae*, *P. aeruginosa*, and *Acinetobacter*, all subjects of this study, and infections are mostly health care associated (32). This report shows that Artilysins can drastically expand the spectrum of endolysins as a novel class of promising anti-infectives (33), making Gram-negative species susceptible to these new enzyme-based antibacterials. The activity of Artilysins in two different settings (*C. elegans* bacterial infection model and keratinocytes) shows that Artilysins may have a potentially broad field of applications ranging from topical, mucosal, and gastrointestinal medical use to disinfection, veterinary, food, feed, and agricultural applications.

MATERIALS AND METHODS

Bacterial strains. *Pseudomonas aeruginosa* PAO1 (ATCC 15692), originally a wound isolate, is now a widely used laboratory strain (34). The clinical *P. aeruginosa* strains Br667, a multiresistant (10 of 11 antibiotics) burn wound isolate collected in the intensive care unit in the Queen Astrid Military Hospital in Brussels, Belgium, PA14, a highly virulent wound isolate from Boston, MA, and other clinical *P. aeruginosa* strains were all provided by J.-P. Pirnay (19, 35). *Pseudomonas putida* G1 was isolated from Russian soil in the neighborhood of Moscow (V. Krylov, Laboratory of Bacteriophage Genetics). *Acinetobacter baumannii* 25 is an uncharacterized clinical isolate from the Queen Astrid Military hospital, donated by Maya Merabishvilli (Lab MCT, Brussels, Belgium), and the *Burkholderia pseudomallei* strain used is a clinical strain from the University Hospital of Gasthuisberg (Leuven, Belgium) isolated by J. Verhaegen (Laboratory of Clinical Microbiology and Mycology, UZ Leuven). *S.* Typhimurium LT2 was provided by the Centre of Food and Microbial Technology (KU Leuven, Belgium). Several different *Escherichia coli* strains were used in this study: *E. coli* XL1-Blue MRF′ (Agilent Technologies, Santa Clara, CA) for antibacterial activity testing, *E. coli* TOP10 (Life Technologies, Carlsbad, CA) for DNA cloning and cell stock storage, and *E. coli* BL21(DE3) pLysS, BL21-CodonPlus-(DE3)-RIL, and BL21-CodonPlus-(DE3)-RP (Agilent Technologies) as host strains for protein expression. For proper selection, ampicillin (Roche Diagnostics, Mannheim, Germany) (100 μg/ml) or chloramphenicol (Calbiochem, Darm-

stadt, Germany) (50 μg/ml) was used. All strains were grown at 37°C, except for *P. putida* G1 (30°C), in lysogeny broth (LB).

Plasmid construction. Overviews of all LPS-destabilizing peptides and produced Artilysins are given in Tables S1 to S3 in the supplemental material and Fig. 1, respectively. Open reading frames (ORFs) encoding the different endolysins were amplified (*Pfu* polymerase; Thermo Fisher Scientific, Waltham, MA) with purified genomic DNA isolated from the respective phages as template DNA. Cloning into the pEXP5CT/TOPO expression vector was performed according to the manufacturer's guidelines (Life Technologies). The polycationic nonapeptide (PCNP) and the hydrophobic pentapeptide (HPP) were fused to endolysins by a standard PCR on purified genomic DNA of the respective phages using forward (N-terminal fusion) or reverse (C-terminal fusion) primers that harbor the peptide-encoding sequence. For N-terminal fusion of the α_4, MW1, MW2, Lycotoxin1, and Parasin1 peptides, an adapted version of the ligation-independent cloning (LIC) technique (36) was used. Briefly, peptide-encoding cassettes, created by hybridization of specific primer pairs (20 μM each), were treated with a mixture of dCTP (Promega, Agora, WI) and T4 DNA polymerase (Thermo Fisher Scientific) to introduce LIC-compatible 5′ sticky ends. In parallel, the endolysin-encoding expression vectors were made LIC compatible by introduction of a unique Ecl136II restriction endonuclease site upstream of the endolysin-encoding ORF using a standard PCR (see intermediate constructs in Table S3 in the supplemental material). The procedure was followed by linearization with Ecl136II endonuclease (New England Biolabs, Ipswich, MA) and creation of complementary sticky ends by treatment with dGTP (Promega) and T4 DNA polymerase. A short incubation step of the hybridized peptide-encoding cassettes with the LIC-compatible vectors completed the cloning process. Two different types of double-tag fusions were constructed in this study: type 1, with the PCNP located N-terminally to the second peptide and the endolysin (type 1 conformation: PCNP—second peptide—endolysin), and type 2, with the PCNP between the second peptide and the endolysin (type 2 conformation: second peptide-PCNP-endolysin). For the type 1 configuration, a standard PCR with a PCNP peptide-encoding 5′ primer (*Pfu* polymerase) was applied on purified pEXP5-CT/α_4-endolysin and pEXP5-CT/HPP-endolysin plasmid DNA, respectively. To obtain type 2 double-tag fusions, the same adapted version of the LIC method was used as described for the single-peptide fusion, except that the pEXP5CT/PCNP-endolysin vector was used as the template. All type 1 and type 2 fusion constructs were introduced in the pEXP5CT-TOPO expression vector. To construct plasmids with extended linkers between the PCNP-encoding sequence and the endolysin-encoding ORF, a standard PCR was first used to introduce NheI and NgoMIV restriction sites for directional cloning. Upon double digestion of the obtained pEXP5CT/PCNP-NheI-NgoMIV-endolysin (for N-terminal end) and pEXP5CT/endolysin-NgoMIV-NheI-PCNP (for C-terminal end) constructs (NgoMIV, New England Biolabs; NheI, Thermo Fisher Scientific), cassettes of various lengths with 5′ complementary sticky ends (encoding the following amino acid sequences: larval stage 1 [L1] = GAGA, L2 = GAGAGAGA, L3 = GAGAGAGAGAGA, L4 = GAGAGAGAGAGAGAGA), obtained through hybridization of specific primer pairs (20 μM each), were inserted in the vectors (T4 ligase; Thermo Fisher Scientific).

Recombinant expression and purification. Recombinant expression of the different constructs was performed in an *E. coli*-based expression system upon induction of exponentially growing cells (optical density at 600 nm [OD_{600}] = 0.6) with 1 mM isopropyl-beta-D-thiogalactopyranoside (IPTG; Thermo Fisher Scientific), unless otherwise stated. Expression conditions (temperature, time, and expression strain) differed depending on the protein to optimize the soluble-expression levels for each construct (see Table S3 in the supplemental material). Expression was stopped by centrifugation (3,900 × *g*, 30 min, 4°C), and the obtained cell pellet was resuspended in a 1/25 vol of lysis buffer (20 mM NaH_2PO_4 [Merck, Darmstadt, Germany]/NaOH, 0.5 M NaCl, pH 7.4). This cell lysate was then subjected to three freeze-thaw cycles (−80°C/22°C) prior to sonication (Vibra-Cell Sonics, Newtown, CT) (8 cycles of a 30-s pulse and 30-s rest; amplitude of 40%). The protein lysate was then filtered through 0.45- and 0.22-μm-pore-size Durapore membrane filters (Millipore, Billerica, MA). Purification of the His_6-tagged fusion proteins was performed on an Aktä fast protein liquid chromatography (FPLC) system (GE Healthcare, Buckinghamshire, United Kingdom) controlled by UNICORN 5.1 software with Ni^{2+}-nitrilotriacetic acid (NTA) columns (HisTrap HP; GE Healthcare) (1 ml). The wash buffer used in the purification process contains a low protein-dependent imidazole concentration (50 to 80 mM) for higher purification stringency (see Table S3). After dialysis to an appropriate buffer, the protein concentration was determined spectrophotometrically in silica cuvettes at a wavelength of 280 nm (Ultraspec III spectrophotometer; GE Healthcare).

Muralytic assay. Outer-membrane-permeabilized cells were used as the substrate (37). Briefly, *P. aeruginosa* PAO1 cells growing in the mid-exponential phase (OD_{600} = 0.6) were spun down (3,900 × *g*, 30 min, 4°C) and subsequently incubated with gentle shaking for exactly 45 min in chloroform-saturated 0.05 M Tris-HCl (pH 7.7). Cells were then washed in a KH_2PO_4/K_2HPO_4 buffer (ionic strength = 80 mM, pH 7.2) to remove residual chloroform and concentrated to an OD_{600} of 1.5. Upon addition of 30 μl of muralytic enzymes (at from 10 to 2,000 nM) to 270 μl of outer-membrane-permeabilized cells, the optical density was measured spectrophotometrically over time at 655 nm using a Microplate Reader 680 system (Bio-Rad). A standardized calculation method to quantify the muralytic activities of lytic enzymes using this assay was described before (38).

Antibacterial assays. Gram-negative cells growing in the mid-exponential phase (OD_{600} = 0.6) were diluted 100-fold in 5 mM HEPES/NaOH (pH 7.4) to a final density of $\pm 10^6$ CFU/ml. Each cell culture (100 μl) was incubated for 30 min at room temperature with 50 μl endolysin/Artilysin dialyzed against phosphate-buffered saline (PBS) (pH 7.4) and 50 μl 5 mM HEPES/NaOH (pH 7.4) buffer or 50 μl 2 mM EDTA-Na_2 (abbreviated as EDTA; final concentration of 0.5 mM) dissolved in the same buffer. After 30 min of incubation, appropriate dilutions of cell suspensions were plated on LB agar in triplicate. Colonies were counted after overnight incubation at 37°C. The antibacterial activity was quantified as the relative inactivation level in log units [$\log_{10}(N_0/N_i)$, with N_0 = initial number of untreated cells and N_i = number of residual cells counted after treatment). The MIC of LoGT-008/ciprofloxacin against *P. aeruginosa* PAO1 and *A. baumannii* 25 in the presence of EDTA in 96-well plates was determined using the broth microdilution method. Cells were diluted according to the McFarland standard in low-salt LB (10 g/liter tryptone, 5 g/liter yeast extract). A dilution series of LoGT-008/ciprofloxacin was added, and the plate was incubated for 18 h at 37°C. All measurements were performed in comparison to a negative control (medium without bacteria) or a positive control (medium without LoGT-008). The MIC was defined as the minimum concentration that completely inhibited bacterial growth.

Time-lapse microscopy. A temperature-controlled (Okolab Ottaviano, Italy) Ti-Eclipse inverted microscope (Nikon, Champigny-sur-Marne, France) equipped with a TI-CT-E motorized condenser and a CoolSnap HQ2 FireWire charge-coupled-device (CCD) camera was used as described previously (39). *P. aeruginosa* PAO1 cells were grown to mid-exponential phase (OD_{600} = 0.6), washed three times with PBS (pH 7.4), and finally concentrated five times by resuspension in PBS–0.5 mM EDTA-Na_2. LoGT-008 was added to reach a final concentration of 0.5 mg/ml. For imaging, samples were placed on a PBS–0.5 mM EDTA–Na_2–agar pad and a cover glass, essentially as described previously (39), and incubated at 37°C. The time between addition of LoGT-008 to the cells and recording was kept as short as possible (~60 s). Images were acquired using NIS-Elements (Nikon), and the resulting pictures were further handled with ImageJ open source software (downloaded from http://rsbweb.nih.gov/ij/) and CorelDRAW X5.

Human keratinocyte assays. Keratinocytes were seeded in coated (1 μg/ml collagen type I for a minimum of 2 h at 37°C) 25-cm^2 vented

culture flasks at 5,000 cells/cm^2 and cultured until more than 90% confluence was reached (supplemented EpiLife medium; 6 days, 37°C, 5% CO_2, and 95% relative humidity). Confluent grown keratinocytes were infected with clinical *P. aeruginosa* PA14 strains at an infectivity dose of 10^5 or 10^7 CFU/ml. At 1 h after infection, both the unmodified and PCNP-modified endolysins (2 μM final concentration) were added together with EDTA (5 μM final concentration) to the keratinocyte cultures. Uninfected keratinocytes and infected but untreated keratinocytes were included as negative controls. After an additional 3 h of incubation, the infection process was stopped by trypsinization of the residual keratinocytes (TrypLE Select recombinant trypsin [Life Technologies]) for 5 min at 37°C and washing in supplemented EpiLife medium. The cell suspensions were collected and centrifuged at 170 × *g* for 10 min. After centrifugation, the cells were resuspended in supplemented EpiLife medium. Keratinocyte viability was microscopically evaluated (Bürker chamber) using trypan blue live/dead staining. Living keratinocytes appeared as colorless cells under the microscope, whereas dead ones became blue due to their disintegrated cell membrane. For evaluation of the antibacterial activity of the *P. aeruginosa* strains, 10-fold dilutions of the keratinocyte culture were plated on LB agar and the residual bacterial CFUs were quantified for each condition after 18 h of incubation at 37°C. The antibacterial activity is expressed in percent reduction relative to the untreated negative control. Multiple pairwise *t* test comparisons were performed ($P < 0.05$) to classify the different conditions in significantly different groups for keratinocyte (bold labels) and bacterial (italic labels) viability.

***C. elegans* infection assay.** *Caenorhabditis elegans* SS104, genotype *glp-4*(*bn2*), was maintained at 16°C on nematode growth medium (NGM) agar covered with a lawn of *E. coli* OP 50 as a feed source (40). Nematode experiments were performed with synchronized L4-stage nematodes acquired by adult bleaching and hatching of the eggs at 16°C for 4 days. For infection of *C. elegans* SS104, 50 synchronized L4-stage nematodes were seeded on bacterial lawns of *P. aeruginosa* PA14. Lawns were prepared by spreading 100 μl of culture at the stationary phase of growth on top of the NGM agar and incubation at 37°C for 18 h before seeding. The infection took place for 24 h at 26°C. Nematode survival after infection was evaluated by the liquid assay as described before (41, 42). Briefly, infected nematodes were washed three times with M9 buffer to remove attached bacteria and transferred to 96-well plates (~10 nematodes per well). Wells contained 100 μl of an NGM/M9 buffer (1:4) mixture, 50 μl (PCNP−) endolysin dialyzed against PBS (pH 7.4), and 50 μl EDTA (0.5 mM final concentration)–PBS (pH 7.4). In addition, PBS buffer (pH 7.4) and EDTA were added as negative controls and ciprofloxacin (Sigma-Aldrich) (5× MIC) as a positive control. Each condition was tested at a 10-fold level. Survival of *C. elegans* SS104 was determined by monitoring the presence or absence of touch-provoked movement for each nematode during 5 subsequent days. Dead nematodes appear as long, immobile rods; living ones move in a sinusoidal shape (41, 42). Multiple pairwise *t* test comparisons were performed ($P < 0.05$) to classify the tested conditions in significantly different groups for *C. elegans* survival after 5 days.

SUPPLEMENTAL MATERIAL

Supplemental material for this article may be found at http://mbio.asm.org/lookup/suppl/doi:10.1128/mBio.01379-14/-/DCSupplemental.

Figure S1, DOCX file, 0.1 MB.
Table S1, DOCX file, 0.1 MB.
Table S2, DOCX file, 0.1 MB.
Table S3, DOCX file, 0.1 MB.
Table S4, DOCX file, 0.1 MB.
Table S5, DOCX file, 0.1 MB.
Table S6, DOCX file, 0.1 MB.
Table S7, DOCX file, 0.1 MB.
Table S8, DOCX file, 0.1 MB.
Table S9, DOCX file, 0.1 MB.

ACKNOWLEDGMENTS

We thank Jean-Pierre Hernalsteens (GEVI, VUB, Brussels) and Karlien Nerinckx for introducing us to the *C. elegans* bacterial infection model.

ARTILYSIN is a registered trademark in the European Union, United States, and other countries.

M.W. held a predoctoral fellowship of the "Instituut voor aanmoediging van Innovatie door Wetenschap en Technologie in Vlaanderen" (IWT Flanders). Y.B. and M.W. were supported by IWT Flanders and Y.B. by a postdoctoral fellowship of the "Bijzonder Onderzoeksfonds—KU Leuven." S.M. is an employee of Lisando GmbH. R.L. acts as scientific adviser to Lisando GmbH.

REFERENCES

1. **Nelson D, Loomis L, Fischetti VA.** 2001. Prevention and elimination of upper respiratory colonization of mice by group A streptococci by using a bacteriophage lytic enzyme. Proc. Natl. Acad. Sci. U. S. A. **98:**4107–4112. http://dx.doi.org/10.1073/pnas.061038398.
2. **Loeffler JM, Nelson D, Fischetti VA.** 2001. Rapid killing of *Streptococcus pneumoniae* with a bacteriophage cell wall hydrolase. Science **294:** 2170–2172. http://dx.doi.org/10.1126/science.1066869.
3. **Schuch R, Nelson D, Fischetti VA.** 2002. A bacteriolytic agent that detects and kills *Bacillus anthracis*. Nature **418:**884–889. http://dx.doi.org/10.1038/nature01026.
4. **Schmelcher M, Powell AM, Becker SC, Camp MJ, Donovan DM.** 2012. Chimeric phage lysins act synergistically with lysostaphin to kill mastitis-causing *Staphylococcus aureus* in murine mammary glands. Appl. Environ. Microbiol. **78:**2297–2305. http://dx.doi.org/10.1128/AEM.07050-11.
5. **Nelson DC, Schmelcher M, Rodriguez-Rubio L, Klumpp J, Pritchard DG, Dong S, Donovan DM.** 2012. Endolysins as antimicrobials. Adv. Virus Res. **83:**299–365. http://dx.doi.org/10.1016/B978-0-12-394438-2.00007-4.
6. **Morita M, Tanji Y, Orito Y, Mizoguchi K, Soejima A, Unno H.** 2001. Functional analysis of antibacterial activity of *Bacillus amyloliquefaciens* phage endolysin against gram-negative bacteria. FEBS Lett. **500:**56–59. http://dx.doi.org/10.1016/S0014-5793(01)02587-X.
7. **Walmagh M, Briers Y, dos Santos SB, Azeredo J, Lavigne R.** 2012. Characterization of modular bacteriophage endolysins from Myoviridae phages OBP, 201φ2-1 and PVP-SE1. PLoS One **7:**e36991. http://dx.doi.org/10.1371/journal.pone.0036991.
8. **Delcour AH.** 2009. Outer membrane permeability and antibiotic resistance. Biochim. Biophys. Acta **1794:**808–816. http://dx.doi.org/10.1016/j.bbapap.2008.11.005.
9. **Briers Y, Cornelissen A, Aertsen A, Hertveldt K, Michiels CW, Volckaert G, Lavigne R.** 2008. Analysis of outer membrane permeability of *Pseudomonas aeruginosa* and bactericidal activity of endolysins KZ144 and EL188 under high hydrostatic pressure. FEMS Microbiol. Lett. **280:** 113–119. http://dx.doi.org/10.1111/j.1574-6968.2007.01051.x.
10. **Briers Y, Walmagh M, Lavigne R.** 2011. Use of bacteriophage endolysin EL188 and outer membrane permeabilizers against *Pseudomonas aeruginosa*. J. Appl. Microbiol. **110:**778–785. http://dx.doi.org/10.1111/j.1365-2672.2010.04931.x.
11. **Lukacik P, Barnard TJ, Keller PW, Chaturvedi KS, Seddiki N, Fairman JW, Noinaj N, Kirby TL, Henderson JP, Steven AC, Hinnebusch BJ, Buchanan SK.** 2012. Structural engineering of a phage lysin that targets gram-negative pathogens. Proc. Natl. Acad. Sci. U. S. A. **109:**9857–9862. http://dx.doi.org/10.1073/pnas.1203472109.
12. **Nikaido H.** 2003. Molecular basis of bacterial outer membrane permeability revisited. Microbiol. Mol. Biol. Rev. **67:**593–656. http://dx.doi.org/10.1128/MMBR.67.4.593-656.2003.
13. **Ibrahim HR, Yamada M, Matsushita K, Kobayashi K, Kato A.** 1994. Enhanced bactericidal action of lysozyme to *Escherichia coli* by inserting a hydrophobic pentapeptide into its C-terminus. J. Biol. Chem. **269:** 5059–5063.
14. **Düring K, Porsch P, Mahn A, Brinkmann O, Gieffers W.** 1999. The non-enzymatic microbicidal activity of lysozymes. FEBS Lett. **449:**93–100.
15. **Park IY, Park CB, Kim MS, Kim SC.** 1998. Parasin I, an antimicrobial peptide derived from histone H2A in the catfish, *Parasilurus asotus*. FEBS Lett. **437:**258–262. http://dx.doi.org/10.1016/S0014-5793(98)01238-1.
16. **Yan L, Adams ME.** 1998. Lycotoxins, antimicrobial peptides from venom of the wolf spider *Lycosa carolinensis*. J. Biol. Chem. **273:**2059–2066. http://dx.doi.org/10.1074/jbc.273.4.2059.

17. **Briers Y, Schmelcher M, Loessner MJ, Hendrix J, Engelborghs Y, Volckaert G, Lavigne R.** 2009. The high-affinity peptidoglycan binding domain of *Pseudomonas* phage endolysin KZ144. Biochem. Biophys. Res. Commun. **383:**187–191. http://dx.doi.org/10.1016/j.bbrc.2009.03.161.
18. **Briers Y, Volckaert G, Cornelissen A, Lagaert S, Michiels CW, Hertveldt K, Lavigne R.** 2007. Muralytic activity and modular structure of the endolysins of *Pseudomonas aeruginosa* bacteriophages phiKZ and EL. Mol. Microbiol. **65:**1334–1344. http://dx.doi.org/10.1111/j.1365-2958.2007.05870.x.
19. **Pirnay JP, De Vos D, Cochez C, Bilocq F, Pirson J, Struelens M, Duinslaeger L, Cornelis P, Zizi M, Vanderkelen A.** 2003. Molecular epidemiology of *Pseudomonas aeruginosa* colonization in a burn unit: persistence of a multidrug-resistant clone and a silver sulfadiazine-resistant clone. J. Clin. Microbiol. **41:**1192–1202. http://dx.doi.org/10.1128/JCM.41.3.1192-1202.2003.
20. **Walmagh M, Boczkowska B, Grymonprez B, Briers Y, Drulis-Kawa Z, Lavigne R.** 2013. Characterization of five novel endolysins from gram-negative infecting bacteriophages. Appl. Microbiol. Biotechnol. **97:**4369–4375. http://dx.doi.org/10.1007/s00253-012-4294-7.
21. **Raetz CR, Whitfield C.** 2002. Lipopolysaccharide endotoxins. Annu. Rev. Biochem. **71:**635–700. http://dx.doi.org/10.1146/annurev.biochem.71.110601.135414.
22. **Church D, Elsayed S, Reid O, Winston B, Lindsay R.** 2006. Burn wound infections. Clin. Microbiol. Rev. **19:**403–434. http://dx.doi.org/10.1128/CMR.19.2.403-434.2006.
23. **De Corte P, Verween G, Verbeken G, Rose T, Jennes S, De Coninck A, Roseeuw D, Vanderkelen A, Kets E, Haddow D, Pirnay JP.** 2012. Feeder layer- and animal product-free culture of neonatal foreskin keratinocytes: improved performance, usability, quality and safety. Cell Tissue Bank. **13:**175–189. http://dx.doi.org/10.1007/s10561-011-9247-3.
24. **Tan MW, Mahajan-Miklos S, Ausubel FM.** 1999. Killing of *Caenorhabditis elegans* by *Pseudomonas aeruginosa* used to model mammalian bacterial pathogenesis. Proc. Natl. Acad. Sci. U. S. A. **96:**715–720. http://dx.doi.org/10.1073/pnas.96.2.715.
25. **Gasson MJ.** April 1991. iral products. US patent 6,083,684A.
26. **Vaara M.** 1992. Agents that increase permeability of the outer membrane. Microbiol. Rev. **56:**395–411.
27. **Kümmerer K.** 2003. Significance of antibiotics in the environment. J. Antimicrob. Chemother. **52:**5–7. http://dx.doi.org/10.1093/jac/dkg293.
28. **Masschalck B, Michiels CW.** 2003. Antimicrobial properties of lysozyme in relation to foodborne vegetative bacteria. Crit. Rev. Microbiol. **29:**191–214. http://dx.doi.org/10.1080/713610448.
29. **Ibrahim HR, Kato A, Kobayashi K.** 1991. Antimicrobial effects of lysozyme against gram-negative bacteria due to covalent binding of palmitic acid. J. Agric. Food Chem. **39:**2077–2082. http://dx.doi.org/10.1021/jf00011a039.
30. **Ibrahim HR, Yamada M, Kobayashi K, Kato A.** 1992. Bactericidal action of lysozyme against gram-negative bacteria due to insertion of a hydrophobic pentapeptide into its C-terminus. Biosci. Biotechnol. Biochem. **56:**1361–1363. http://dx.doi.org/10.1271/bbb.56.1361.
31. **Ibrahim HR, Kobayahsi K, Kato A.** 1993. Length of hydrocarbon chain and antimicrobial action to gram-negative bacteria of fatty acylated lysozyme. J. Agric. Food Chem. **41:**1164–1168. http://dx.doi.org/10.1021/jf00031a029.
32. **Centers for Disease Control and Prevention, CDC.** 2013. Antibiotic resistance threats in the United States. http://www.cdc.gov/drugresistance/threat-report-2013/pdf/ar-threats-2013-508.pdf. Accessed: 10 February 2014.
33. **Pastagia M, Schuch R, Fischetti VA, Huang DB.** 2013. Lysins: the arrival of pathogen-directed anti-infectives. J. Med. Microbiol. **62:**1506–1516.
34. **Holloway BW.** 1955. Genetic recombination in *Pseudomonas aeruginosa*. J. Gen. Microbiol. **13:**572–581. http://dx.doi.org/10.1099/00221287-13-3-572.
35. **Pirnay JP, Bilocq F, Pot B, Cornelis P, Zizi M, Van Eldere J, Deschaght P, Vaneechoutte M, Jennes S, Pitt T, De Vos D.** 2009. *Pseudomonas aeruginosa* population structure revisited. PLoS One **4:**e7740. http://dx.doi.org/10.1371/journal.pone.0007740.
36. **Haun RS, Serventi IM, Moss J.** 1992. Rapid, reliable ligation-independent cloning of PCR products using modified plasmid vectors. BioTechniques **13:**515–518.
37. **Lavigne R, Briers Y, Hertveldt K, Robben J, Volckaert G.** 2004. Identification and characterization of a highly thermostable bacteriophage lysozyme. Cell. Mol. Life Sci. **61:**2753–2759. http://dx.doi.org/10.1007/s00018-004-4301-y.
38. **Briers Y, Lavigne R, Volckaert G, Hertveldt K.** 2007. A standardized approach for accurate quantification of murein hydrolase activity in high-throughput assays. J. Biochem. Biophys. Methods **70:**531–533. http://dx.doi.org/10.1016/j.jbbm.2006.10.009.
39. **Cenens W, Mebrhatu MT, Makumi A, Ceyssens PJ, Lavigne R, Van Houdt R, Taddei F, Aertsen A.** 2013. Expression of a novel P22 ORFan gene reveals the phage carrier state in *Salmonella typhimurium*. PLoS Genet. **9:**e1003269. http://dx.doi.org/10.1371/journal.pgen.1003269.
40. **Brenner S.** 1974. The genetics of *Caenorhabditis elegans*. Genetics **77:**71–94.
41. **Stiernagle T. 11 February** 2006. Maintenance of *C. elegans*. *In* The *C. elegans* Research Community, WormBook. http://dx.doi.org/10.1895/wormbook.1.101.1.
42. **Moy TI, Ball AR, Anklesaria Z, Casadei G, Lewis K, Ausubel FM.** 2006. Identification of novel antimicrobials using a live-animal infection model. Proc. Natl. Acad. Sci. U. S. A. **103:**10414–10419. http://dx.doi.org/10.1073/pnas.0604055103.